

Article

Effect of the Flagellar Gene *fliL* on the Virulence of *Pseudomonas plecoglossicida* to Hybrid Grouper (*Epinephelus fuscoguttatus* ♀ × *E. lanceolatus* ♂)

Lian Shi ¹, Junjie Zhang ², Lingmin Zhao ¹, Qi Li ¹ , Lixing Huang ¹, Yingxue Qin ¹ and Qingpi Yan ^{1,*} 

¹ Fisheries College, Jimei University, Xiamen 361021, China; shilian_work@126.com (L.S.); yxqin@jmu.edu.cn (Y.Q.)

² College of Life Science, Xinjiang Agricultural University, Urumqi 830052, China; zhangjuji@sina.cn

* Correspondence: yanqp@jmu.edu.cn

Abstract: *Pseudomonas plecoglossicida* is the pathogen of visceral white spot disease in marine fish, which usually occurs at 16–19 °C and has resulted in heavy economic losses. Our previous RNA sequencing revealed that the expression of the *fliL* gene in *P. plecoglossicida* was significantly up-regulated during infection of the host. In order to study the influence of the *fliL* gene on the virulence of *P. plecoglossicida*, the *fliL* gene of the NZBD9 strain was knocked out by the homologous recombination method, the *fliL* gene-deleted strain ($\Delta fliL$ strain) constructed, and complemented the *fliL* gene to the $\Delta fliL$ strain to obtain the C- $\Delta fliL$ strain. The growth curves of the NZBD9 strain, $\Delta fliL$ strain, and C- $\Delta fliL$ strain did not show significant differences. Compared with the NZBD9 strain, the motility, adhesion, and biofilm formation ability were tendered in the $\Delta fliL$ strain ($p < 0.05$); the complement of the *fliL* gene enhanced these abilities to the level of the NZBD9 strain. The results of artificial infection experiments showed that the LD₅₀ of NZBD9 strain, $\Delta fliL$ strain, and C- $\Delta fliL$ strain in hybrid grouper (*Epinephelus fuscoguttatus* ♀ × *E. lanceolatus* ♂) were 5.0×10^3 CFU/fish, 6.3×10^4 CFU/fish, and 1.3×10^3 CFU/fish, respectively. RNA sequencing was performed on wild-type strains and $\Delta fliL$ strains. A total of 126 differentially expressed genes (DEGs) were screened ($p < 0.05$), of which 114 were downregulated and 12 were upcontrolled, among which several genes related to the six-type secretion system and transport activity were significantly downregulated. The DEGs were aligned to the GO and KEGG databases and enriched to 44 GO pathways and 39 KEGG pathways, respectively. The active pathways of ABC transporters were significantly enriched in both databases. These results indicate that the *fliL* gene is related to the movement, biofilm formation, and adhesion ability of *P. plecoglossicida*, and may reduce virulence by affecting substance transport and bacterial secretion.

Keywords: *Pseudomonas plecoglossicida*; *fliL*; virulence; transcriptome

Key Contribution: The *fliL* gene might be influencing the *P. plecoglossicida*'s system of material transportation and flagellum assembly to reduce its virulence.



Citation: Shi, L.; Zhang, J.; Zhao, L.; Li, Q.; Huang, L.; Qin, Y.; Yan, Q. Effect of the Flagellar Gene *fliL* on the Virulence of *Pseudomonas plecoglossicida* to Hybrid Grouper (*Epinephelus fuscoguttatus* ♀ × *E. lanceolatus* ♂). *Fishes* **2023**, *8*, 397. <https://doi.org/10.3390/fishes8080397>

Academic Editor: Bei Wang

Received: 9 June 2023

Revised: 21 July 2023

Accepted: 24 July 2023

Published: 1 August 2023



Copyright: © 2023 by the authors. Licensee MDPI, Basel, Switzerland. This article is an open access article distributed under the terms and conditions of the Creative Commons Attribution (CC BY) license (<https://creativecommons.org/licenses/by/4.0/>).

1. Introduction

With the vigorous development of the mariculture industry, especially the promotion of a high-density aquaculture model, the frequency and range of aquatic diseases caused by bacteria have gradually increased [1–3]. Marine and freshwater fish diseases caused by *Vibrio*, *Pseudomonas*, and *Aeromonas* are more common, causing serious losses to aquaculture [4–7]. Pathogenic *Pseudomonas plecoglossicida* was first isolated and identified as a new strain in ayu (*Plecoglossus altivelis*) suffering from bacterial haemorrhagic ascites from Japan in 2000 [8]. In recent years, reports have revealed that this pathogen can cause infection in a wide variety of fish, including crucian carp (*Carassius auratus*), rainbow trout (*Oncorhynchus mykiss*), large yellow croaker (*Larimichthys crocea*), and orange-spotted

grouper (*Epinephelus coioides*), causing high mortality and posing a great threat to aquaculture [9–11]. Previous research in our laboratory found that many genes were involved in regulating the virulence of *P. plecoglossicida*. The *rpoD* (RNA polymerase sigma factor) gene was found to be a key virulence gene in the process of infecting grouper [12], and *fliG* (flagellar motor switch protein, *fliG*), *flgC* (flagellar basal-body rod protein, *flgC*), *exbB* (biopolymer transport gene), and other genes also made great contributions to the infection of orange-spotted grouper [13–15]. However, the pathogenesis of bacterial diseases is an extremely complex process, and the virulence of *P. plecoglossicida* is not well understood. Based on the early transcriptome data of our laboratory (NCBI, SRP115064), the results showed that the *fliL* gene was significantly overexpressed in the spleen of orange-spotted grouper infected with the wild-type *P. plecoglossicida* strain NZBD9. It is speculated that this gene is related to the virulence of *P. plecoglossicida*.

Most bacteria migrate to a favorable living environment by rotating flagella/flagella [16]. In this process, torque is generated by the flagella motor to provide rotational power for the flagella filament [17]. FliL (flagellar basal body-associated FliL family protein) is a single-transmembrane protein (IM protein) associated with flagellar motor function [18], close to the flagellar basal body [19]. Studies have shown that the interaction of FliL with the rotor (MS ring) and stator (MotA and MotB) enhances the flagellar motor torque, thereby maintaining the integrity and stability of the flagellar rod [19–22]. Motility mainly plays a role in the early stage of bacterial infection [23]. Studies have found that *fliL* is essential for the movement of *Rhodobacter sphaericum*, and in the absence of the *fliL* gene, flagella rotation is seriously damaged [24]. In *Vibrio alginolyticus*, loss of *fliL* will not affect cell morphology or flagella, but it will lead to a significant decrease in swimming speed under a high load. Therefore, *fliL* is very important to generate torque under high-load conditions [16]. Moreover, it is reported that FliL is related to the swimming or adhesion mechanisms of *Clostridium difficile*, and the loss of the *fliL* gene may affect the cell's ability to perceive the surface [19]. However, research on the function of the *fliL* gene in *P. plecoglossicida* has not been published yet.

In this study, a two-step allele exchange method was used to construct an unmarked deletion strain of the *fliL* gene ($\Delta fliL$ strain) and a complement strain of $\Delta fliL$ (C- $\Delta fliL$ strain) of *P. plecoglossicida* with reference to the previous method [25]. Meanwhile, a *fliL* gene complement strain was constructed. In order to study the effect of the *fliL* gene on the pathogenicity of bacteria, the biological characteristics and virulence tests were carried out on the deleted and supplemented strains. In addition, to further elucidate the potential mechanism of virulence of the *fliL* gene, the transcriptomes of the NZBD9 strain, the *fliL* gene deletion strain of *P. plecoglossicida* were compared and analyzed.

2. Materials and Methods

2.1. Bacterial Strains and Culture Conditions

The strains used in this experiment were all *P. plecoglossicida*, in which the wild-type strain NZBD9 was isolated from the spleen of diseased, large yellow croaker. The $\Delta fliL$ strain was obtained by the knockout *fliL* gene of the wild strain, and the C- $\Delta fliL$ strain was obtained by complementing the *fliL* gene to the $\Delta fliL$ strain. All three strains were grown in Luria-Bertani (LB) medium at 18 °C or 28 °C with 220 r/min (NZBD9, $\Delta fliL$ containing 100 µg/mL ampicillin, and C- $\Delta fliL$ adding 10 µg/mL tetracycline.). *Escherichia coli* Top10 and DH5 α were obtained from TransGen Biotech (Beijing, China) and cultured in LB broth at 37 °C with 220 r/min. The plasmid pK18mobsacB and pCM130/tac located in DH5 α were preserved in our laboratory and cultured in LB broth at 37 °C with 220 r/min.

2.2. Construction of Deletion and Complement Strains

2.2.1. Construct the $\Delta fliL$ Strain

According to the genome sequence of the NZBD9 strain (NCBI, PHNR00000000), primers P₁P₂ and P₃P₄ were designed (primers' sequence is shown in Supplementary Table S1) to amplify the upstream and downstream homologous fragment (about 800 bp) of the *fliL* gene,

respectively, and the fusion fragment (about 1600 bp) was obtained by running overlapping PCR (P_1/P_4 primers). The PCR amplification procedure was as follows: 95 °C for 4 min; 30 cycles of 95 °C for 30 s, 56 °C for 30 s, and 72 °C for 1 min; and 72 °C for 5 min. The fusion fragment ($\Delta fliL$) and plasmid pK18mobsacB were digested with restriction enzymes *EcoR* I and *Xba* I (Takara Biotech, Beijing, China), respectively, (water bath at 37 °C for 5 h), and T4 ligase (Takara Biotech, China) was added for connection (16 °C for 5 h) [25]. Then, the ligation product was transformed into Top10 receptive cells of *E. coli* by heat shock, and the recombinant plasmid pK18mobsacB- $\Delta fliL$ was screened with LB agar (50 µg/mL Kan). After enzyme digestion and sequencing (Shanghai Shengong Bioengineering Co., Ltd., Shanghai, China), the correct recombinant plasmid was transformed into the susceptible cells of the NZBD9 strain by electroporation with 2.5 kV (MicroPulser™, BIO-RAD, Mountain View, CA, USA), and the successful transformants were screened out by Kan (25 µg/mL). After dilution, the transformant was spread onto LB agar plates containing 10% sucrose until a single colony grew [26]. Then, single colonies that could grow in ampicillin but could not grow in Kan were screened; P_1/P_4 primers were used to PCR isolated colonies, and the wild-type strain was used as a positive control. The PCR amplification procedure was the same as above. The strain that can amplify the fusion fragment (about 1600 bp) is the strain that has lost the *fliL* gene ($\Delta fliL$ strain).

2.2.2. Construction of the Complement Strain C- $\Delta fliL$

According to the *fliL* gene sequence of the NZBD9 strain and the enzyme restriction site of plasmid pCM130/tac, the primers C- $\Delta fliL$ -F/R were designed (primers' sequence is shown in Table S1). The complete *fliL* gene fragment was amplified by PCR with the DNA of the NZBD9 strain as a template. The PCR amplification procedure was as follows: 95 °C for 4 min; 30 cycles of 95 °C for 30 s, 58 °C for 30 s, and 72 °C for 30 s; and 72 °C for 5 min. The gene fragment and plasmid pCM130/tac were digested with *BsrG* I and *Nsi* I (New England Biolabs, Ipswich, MA, USA) enzymes (water bath at 37 °C for 5 h), and T4 ligase was added for connection (16 °C for 5 h). Then, the ligation product was transformed into DH5 α receptive cells of *E. coli* by heat shock, and the recombinant plasmid pCM130/tac-*fliL* was screened with LB agar (10 µg/mL tetracycline). The receptor cells of the $\Delta fliL$ strain were prepared, and the recombinant plasmid was shocked (2.5 kV) into them. The $\Delta fliL$ strain cells with recombinant plasmid were inoculated on an LB agar plate containing 10 µg/mL tetracycline and incubated under 18 °C. A single colony was selected and cultured in LB broth (containing 10 µg/mL tetracycline) for colony PCR verification. The sequence of all primers used is shown in Supplementary Table S1.

2.3. Validation of mRNA Levels of Deletion and Complement Strains

The genomes of the NZBD9 strain, $\Delta fliL$ strain, and C- $\Delta fliL$ strain were extracted using the bacterial genome DNA kit (TransGen Biotech, Beijing, China). The internal primer P_5/P_6 (Table S1) of the *fliL* gene was designed as the verification primer and subjected to PCR. The PCR amplification procedure was as follows: 95 °C for 4 min; 30 cycles of 95 °C for 30 s, 52 °C for 30 s, and 72 °C for 30 s; and 72 °C for 5 min. To verify the expression of the *fliL* gene at the mRNA level, total bacterial RNA was extracted with TRIzol reagent. According to the manufacturer's protocols, the cDNA was synthesized using TransScript All-in-One First-Strand cDNA Synthesis SuperMix for qRT-PCR (One-Step gDNA Removal) (Transgenic Biotechnology Company, Beijing, China). The temperature was set to 42 °C for 15 min and 85 °C for 5 s. Compared with the NZBD9 strain, the qRT-PCR based on the method of SYBR Green, was used to run the relative gene expression quantitatively, and the relative gene expression level was calculated by the $2^{-\Delta\Delta CT}$ method. The primer of the *fliL* gene and the endogenous gene 16S rDNA was designed by Primer Premier 5.0, and the sequence is shown in Supplementary Table S1. Three samples were in each group, and for each sample, three replicates were performed.

2.4. Determination of Growth Curve

The NZBD9 strain, Δ *fliL* strain, and C- Δ *fliL* strain of *P. plecoglossicida* were cultured in LB broth at 18 °C with shaking at 220 r/min overnight to $OD_{600} = 0.5$, and then diluted with sterile LB broth to $OD_{600} = 0.2 \pm 0.01$. The bacterial suspension was diluted 100,000 times with sterile LB broth, and 200 μ L was added into 96-well plates after mixing evenly. There were 12 replicates for each strain, and 200 μ L LB broth with 12 wells used for control group. The OD value at 600 nm was measured at 18 °C with a multifunctional microtiter plate detector (every 30 min for 48 h).

2.5. Motility Measurement

The motility assay of *P. plecoglossicida* was carried out according to the method of Yang et al. [15] with some modifications. The NZBD9 strain, Δ *fliL* strain, and C- Δ *fliL* strain were cultured in LB broth, and overnight cultured at 18 °C with shaking at 220 r/min until $OD_{600} = 0.2$. One μ L bacterial suspension was inoculated on an LB semi-solid plate containing 0.4% agar and cultured at 18 °C for 24 h. The colonies were then photographed and the diameter of each colony was determined. Three independent biological repeats were set up for the detection of each strain, and each repeat included three technical repeats.

2.6. Determination of Bacterial Adhesion Ability

2.6.1. Preparation of Surface Mucus

Vigorous pearl gentian grouper with no parasites and wounds on the body surface was obtained from a farm without a recent history of the epidemic in Xiamen (Fujian, China). The method of Jiao et al. [14] was followed and slightly modified. We rinsed the surface of the fish with sterile PBS, gently scraped off the mucus on the surface of the fish with clean slides, and mixed well in PBS. The mucus was placed overnight at 4 °C and centrifuged for 30 min twice at $4000 \times g$ and 4 °C. The supernatants were sterilized by filtration using filters with pore sizes of 0.45- μ m and 0.22- μ m successively. The mucus' protein concentration was adjusted to 1 mg protein/mL with PBS according to the Bradford Protein Assay Kit (Solarbio[®], Beijing, China).

2.6.2. In Vitro Adhesion Experiment

In vitro adhesion was determined following a previous study [11]. Some 20 μ L of mucus (1 mg protein/mL) was evenly coated onto a 22 mm² glass slide area and fixed with methanol for 20 min. A total of 200 μ L of a bacterial suspension ($OD_{600} = 0.3 \pm 0.01$) was spotted on a mucus-coated glass slide. Then, the glass slides were placed in a humidified chamber, incubated at 18 °C for 2 h, and then washed five times in PBS (0.01 mol/L, pH = 7.2). Finally, the bacteria were fixed with 4% methanol for 30 min, stained with 1% crystal violet for 3 min, and counted under a microscope ($\times 1000$) (Leica DM4000 B LED, Leica, Wetzlar, Germany). Five glass slides were performed per strain, and the adhered bacteria in 20 randomly selected fields were counted per slide.

2.7. Biofilm Determination

Biofilm formation was explored following previous research [11] with some modifications. Overnight cultures of *P. plecoglossicida* were adjusted to $OD_{600} = 0.2 \pm 0.01$ in LB broth. The bacterial suspension (100 μ L) was added to the wells of 96-well plates (ten wells per strain) and incubated at 18 °C for 24 h. Then, each well was washed gently twice with PBS (2 mL), dyed with 120 μ L of crystal violet (0.1%) for 15 min, gently washed twice with sterile PBS, and air dried. Finally, 200 μ L of acetic acid (33%) was added to each well to dissolve the stained biofilm for 30 min, and OD_{590} of each well was determined using a SYNERGY H1 microplate reader (BioTek, Winooski, VT, USA).

2.8. Measurement of the Chemotactic Response

The assay was accomplished in accordance with the previous method [12]. The *P. plecoglossicida* NZBD9, $\Delta fliL$, and C- $\Delta fliL$ strains were cultured in sterile LB broth medium at 18 °C until an OD600 of about 0.5. The bacteria were adjusted to OD600 = 1.0 using sterile PBS. One end of the mucus-filled capillary tube (inner diameter 0.1 mm, the other end sealed) was immersed in a syringe containing bacterial suspension (250 μ L) and incubated at 18 °C for 1 h. Sterile PBS was applied as a blank control. The bacteria–mucus mixtures in the capillary were diluted into 995 μ L PBS for serial dilution, and 100 μ L bacterial suspension per gradient was coated on an LB agar plate to calculate CFU. Three replicates were set up for each strain.

2.9. Half Lethal Dose (LD₅₀) Test for *P. plecoglossicida*

Healthy weight-match pearl gentian grouper were temporarily cultured in clean and sterile seawater (temperature controlled at 18 \pm 1 °C) for one week. After the fish adapted to recirculating aquaculture, the infection test was carried out. Grouping was set according to the reported method [27]. A total of 160 pearl gentian grouper were randomly divided into 16 groups; each group contained 10 fish, including 5 groups of NZBD9 strain, $\Delta fliL$ strain, and C- $\Delta fliL$ strain, plus a set of negative control (PBS). The intravitreal injection dose of the bacterial solution was set to 5 \times 10⁶, 5 \times 10⁵, 5 \times 10⁴, 5 \times 10³, and 5 \times 10² CFU/fish. The fish injected with 0.2 mL PBS was used as the negative control. The death of the injected fish was observed every 12 h after injection, and the dead fish were removed every time.

2.10. Transcriptomic Analysis

2.10.1. Library Preparation and Sequencing

Overnight cultures of the NZBD9 strain and $\Delta fliL$ strain were centrifuged (4 °C, 4000 \times g, 15 min), and the bacteria were collected for RNA sequencing. Three samples were prepared for each strain as independent biological replicates. The concentration and purity of bacteria total RNA extracted from the sample were detected by Nanodrop2000. The TruSeq™ total RNA library preparation kit was used to construct a library with an initial total RNA volume of 2 μ g.

In the synthesis of the second strand of cDNA, dTTP was replaced by dUTP, and the second strand was degraded by adding the UNG enzyme (Illumina, San Diego, CA, USA). The enriched library was amplified by PCR and quantified by TBS380 (Picogreen). The constructed RNA-seq libraries were sequenced on the Illumina NovaSeq 6000 sequencing platform [28] by Shanghai Majorbio Biomedical Technology Co., Ltd. (Shanghai, China).

2.10.2. Raw Data Statistics and Quality Control

Using statistical methods, the base distribution and quality fluctuation of all sequencing readings in each cycle were counted to obtain raw data. Illumina HiSeq original data contained junction sequences, reads of low quality, sequences with high N-rates, and excessively short sequences, which would affect subsequent sequence assembly. Therefore, the original sequencing data was filtered to obtain high-quality sequencing data (clean data) to ensure the smooth conduct of subsequent analyses. The method was as follows: remove the adapter sequence in reads and 5'-end contains non-A, G, C, T base. The ends of the reads with a quality value less than Q20 were trimmed, the reads with 10% N content were removed, and the small fragments with a length of less than 25 bp were discarded. The FASTX-Toolkit v0.0.14 (http://hannonlab.cshl.edu/fastx_toolkit/ accessed on 22 December 2022) was used to analyze the Illumina raw sequencing data as well as library construction and sequencing quality. SeqPrep (<https://github.com/jstjohn/SeqPrep> accessed on 22 December 2022) was used to perform quality control of the raw sequencing data to obtain high-quality clean data to ensure the accuracy of subsequent analyses.

2.10.3. Comparison with Reference Genome

Clean data (reads) was compared by software based on the Burrows–Wheeler method, and mapped data (reads) was obtained for subsequent analysis. The sequence was indexed by classification and transformation characteristic matrix and compared with the reference genome (NCBI, GCA_003391255-1) with the software of Bowtie (<http://bowtie-bio.sourceforge.net/index.shtml>, accessed on 22 December 2022).

2.10.4. Differentially Expressed Genes (DEGs) and Enrichment Analysis

The gene expression levels were quantitatively analyzed by RSEM software based on one million transcripts (TPM). DESeq2 software was used to analyze the differentially expressed genes (DEGs) between the groups, and the significance screening level was $p\text{-adjust} < 0.05$ and $|\log_2\text{FC}| \geq 1$. GOATOOLS (<https://files.pythonhosted.org/packages/>, accessed on 24 December 2022) and R script were used for GO and KEGG Pathway enrichment analysis of DEGs, and the Fisher precise test was used for calculation. In GO enrichment analysis, the Bonferroni method was used to correct the p value, and the corrected p value (FDR) was < 0.05 , indicating that the GO function was significantly enriched. For KEGG Pathway enrichment analysis, BH (Benjamini and Hochberg) was selected to correct the p value. The corrected p value (FDR) was set to 0.05 as the threshold, and $\text{FDR} < 0.05$ was considered significant enrichment.

2.10.5. Validation of Transcriptome Data

To confirm the reliability of transcriptome data, several upregulated and downregulated genes were randomly selected from RNA-seq results for qRT-PCR validation. The sequence of gene primers is shown in Supplementary Table S2. The 16S rDNA (Table S1) was used as the internal reference gene, and the $2^{-\Delta\Delta\text{CT}}$ method was used for data processing. Three samples were in each group, and for each sample, three replicates were performed.

2.11. Data Analysis

All data were the average standard deviation (SD) of three independent experiments. The data were analyzed by IBM SPSS Statistics v 26.0, and the Dunnett test was used for one-way ANOVA. The p value < 0.05 was indicated as statistically significant.

2.12. Data Access

The RNA-seq data were stored in the GenBank SRA database with entry numbers SRP423148 (NZBD9 strain group) and SRP428021 (ΔfliL strain group).

3. Results

3.1. Construction of *fliL* Gene Deletion and Replacement Strain of *P. plecoglossicida*

The results of the construction process of ΔfliL and $\text{C-}\Delta\text{fliL}$ strains are shown in Supplementary Figures S1 and S2. As shown in Figure 1A, the ΔfliL strain did not exhibit the fragment of the *fliL* gene (468 bp), while both the NZBD9 strain and $\text{C-}\Delta\text{fliL}$ strain exhibited the fragment. Through further verification (mRNA level), as shown in Figure 1B, compared with the wild-type strain, the ΔfliL strain was almost unexpressed, while the $\text{C-}\Delta\text{fliL}$ strain showed an upregulated expression. These results demonstrate that the *fliL* gene deletion strain and complement strain of *P. plecoglossicida* was successfully constructed and can be used in subsequent experiments.

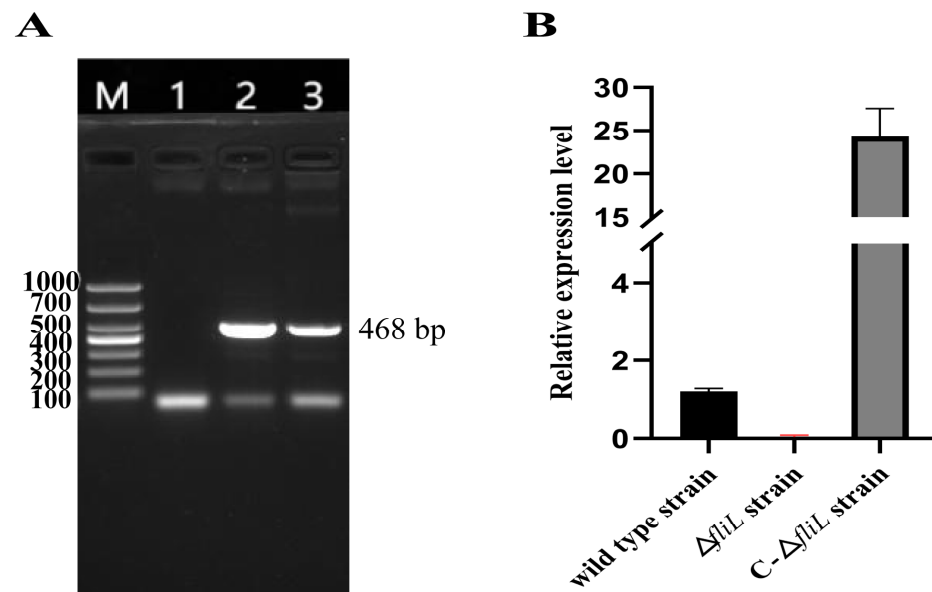


Figure 1. Verification of $\Delta fliL$ and C- $\Delta fliL$ strain of *P. plecoglossicida*. (A) Detection of *fliL* DNA fragment (P_5/P_6 primers), M: DL1000 DNA Marker; 1: DNA of $\Delta fliL$ strain as a template; 2: DNA of C- $\Delta fliL$ strain as a template; 3: DNA of NZBD9 strain as a template; (B) *fliL* gene mRNA levels in three strains of *P. plecoglossicida*. Data were represented by mean + SD ($n = 3$).

3.2. Effect of the *fliL* Gene on the Phenotype of *P. plecoglossicida*

The results of the growth curve (Figure 2A) show that there was no significant difference between the growth of the wild-type strain, $\Delta fliL$, and C- $\Delta fliL$ strain. The motility of the three strains was determined on LB soft agar. Figure 2B shows that the colony diameter of the $\Delta fliL$ strain (10.14 ± 0.85 mm, $p < 0.01$) was significantly smaller than that of the wild strain (11.92 ± 0.52 mm), and the motility of the C- $\Delta fliL$ strain (11.73 ± 0.66 mm) was restored to the state of the wild type. The comparison of biofilm formation indicated that the biofilm color of the $\Delta fliL$ strain was the lightest among the three strains, and the OD₅₉₀ value of the $\Delta fliL$ strain (1.22 ± 0.08 , $p < 0.01$) was significantly lower than that of the wild strain (1.57 ± 0.19) and the C- $\Delta fliL$ strain (1.37 ± 0.08) (Figure 2D). Similarly, the adhesion of the $\Delta fliL$ strain decreased. The number of $\Delta fliL$ strain bacteria attached to the mucus-coated slide was significantly less than that of the wild strain ($p < 0.05$) under the same visual field (Figure 2E,F). As shown in Figure 2C, the chemotactic ability of the $\Delta fliL$ strain was weaker than that of the wild strain, but there was no significant difference.

3.3. Effect of the *fliL* Gene on the Virulence of *P. plecoglossicida*

Mortality (within 7 days) of artificial infection of pearl gentian grouper with *P. plecoglossicida* is presented in Table 1. No fish in the PBS group died during animal testing. Kohl's [29] modified method was used to calculate the LD₅₀ of the wild-type strain, $\Delta fliL$ strain, and C- $\Delta fliL$ strain, with values of 5.0×10^3 CFU/fish (2.1×10^3 – 1.2×10^4 , 95% confidence interval), 6.3×10^4 CFU/fish (1.9×10^4 – 2.1×10^5 , 95% confidence interval), and 1.3×10^3 CFU/fish (4.8×10^2 – 3.7×10^3 , 95% confidence interval), respectively. The result showed that the virulence of the $\Delta fliL$ strain was twelve-fold lower than that of the wild-type strain, while that of the C- $\Delta fliL$ strain was four-fold higher.

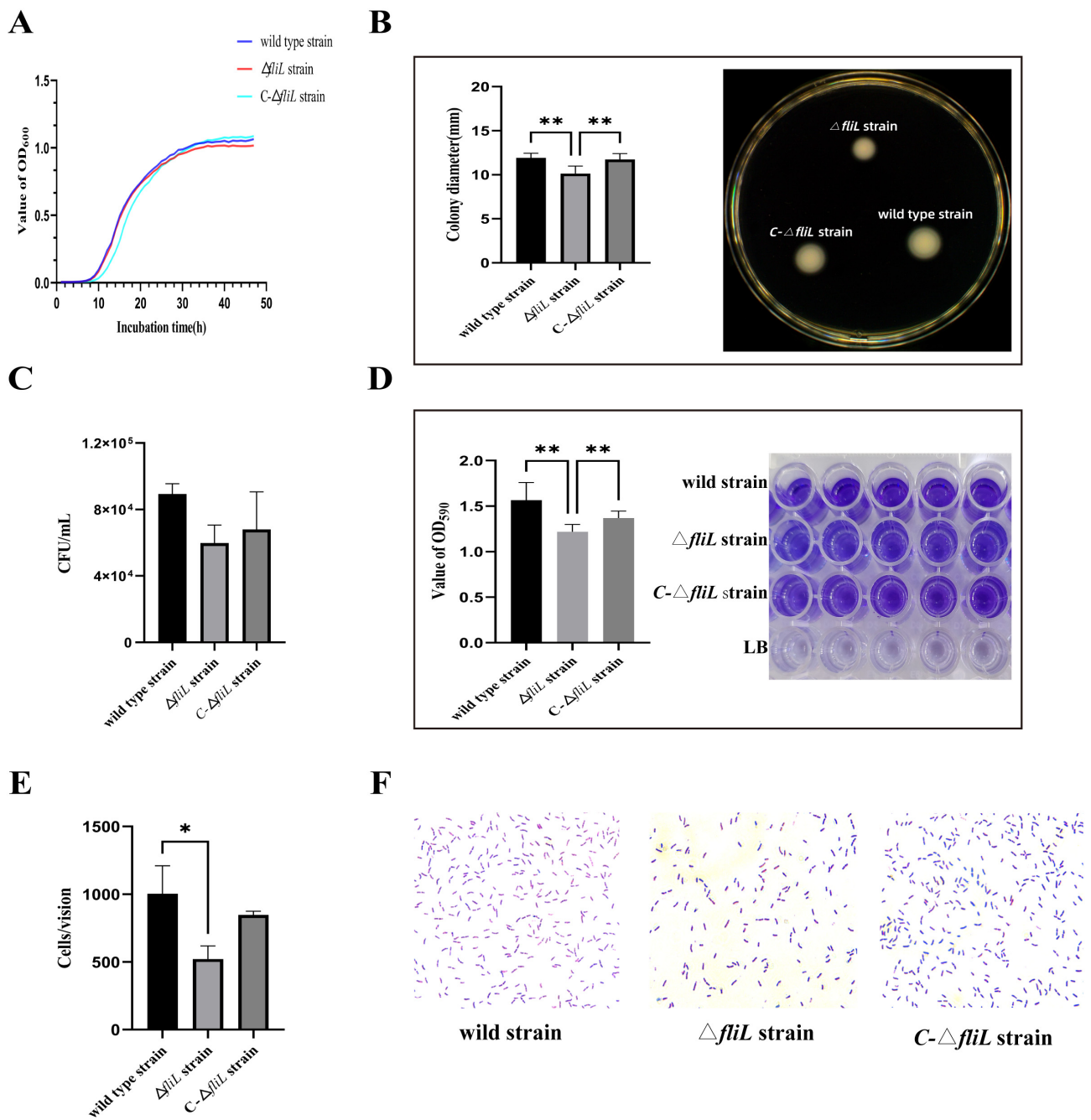


Figure 2. Comparison of the phenotype between different strains of *P. plecoglossicida*. (A) Growth curve; (B) Motility, left: measurement of colony diameter, right: photograph of colony morphology; (C) Chemotaxis; (D) Biofilm formation capacity, left: measurement of OD₅₉₀ value, right: comparison of biofilm colors; (E) The average number of adherent bacteria; (F) Adherence of bacterial cells under the microscope ($\times 1000$). Data were mean \pm SD of different assays with different biological replicates, * $p < 0.05$, ** $p < 0.01$.

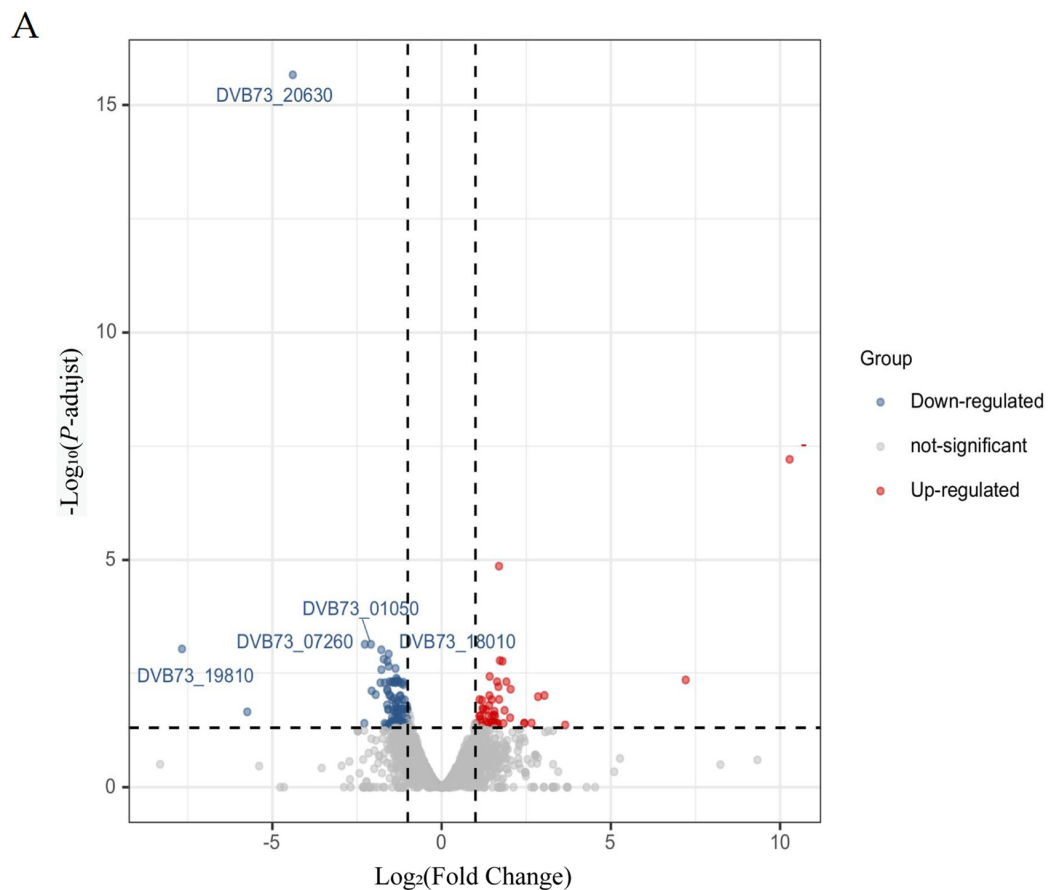
Table 1. Results of the artificial infection of different strains of *P. plecoglossida* to pearl gentian grouper.

Dose (CFU/Fish)	The Number of Test Animals	Wild Type Strain		Δ <i>fliL</i> Strain		C- Δ <i>fliL</i> Strain	
		The Number of Dead	Mortality/%	The Number of Dead	Mortality/%	The Number of Dead	Mortality/%
5×10^6	10	10	100	10	100	10	100
5×10^5	10	10	100	7	70	10	100
5×10^4	10	9	90	4	40	9	90
5×10^3	10	6	60	3	30	8	80
5×10^2	10	0	0	0	0	3	30

3.4. Effect of Knockout of *fliL* Gene on Transcriptome of Wild Strain of *P. plecoglossida*

Judging from the quality of quality-controlled sequence data, the base distribution of each sample is relatively concentrated, with N% approaching 0%. The Q20 (percentage of bases with mass value ≥ 20) and Q30 (percentage of bases with mass value ≥ 30) of each sample were greater than 98.5% and 95.5%. The sequencing error rate was less than 0.1%, indicating the high quality of transcriptome sequencing results. The ratio of clean reads (mapped reads) to the reference genome was more than 98%, which indicated that the selected reference genome assembly could meet the needs of information analysis.

The analysis found that there were 126 DEGs between the transcriptome of the Δ *fliL* strain and wild-type strain, including 114 downregulated genes and 12 upregulated genes (Figure 3A). The first 50 differentially expressed genes were selected for thermographic analysis (Supplementary Figure S3). Five upregulated and downregulated genes were selected for qRT-PCR detection. The trend of gene expression in qRT-PCR results was consistent with sequencing results (Figure 4), which indicated the reliability of transcriptome data.

**Figure 3.** Cont.

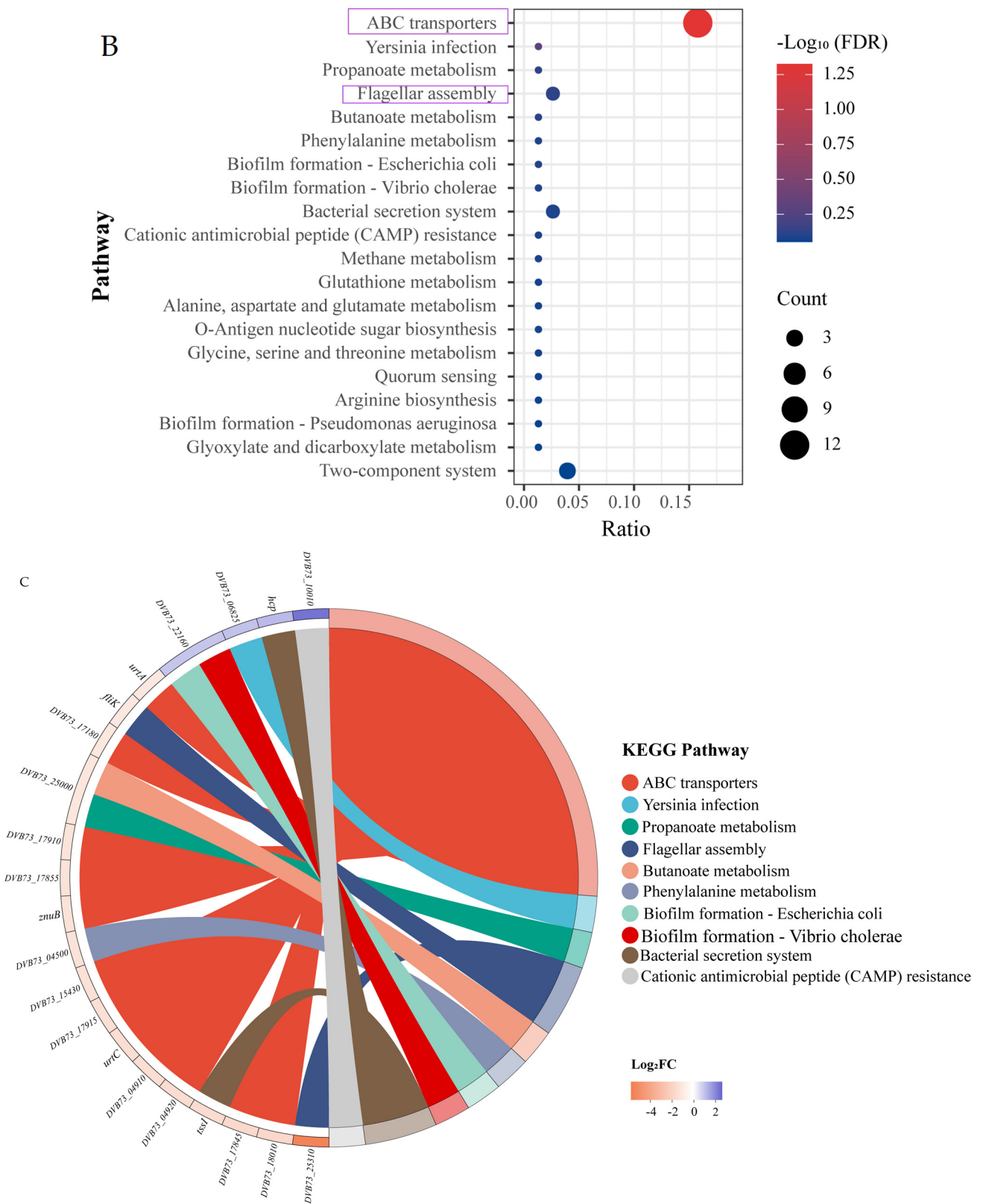


Figure 3. Cont.

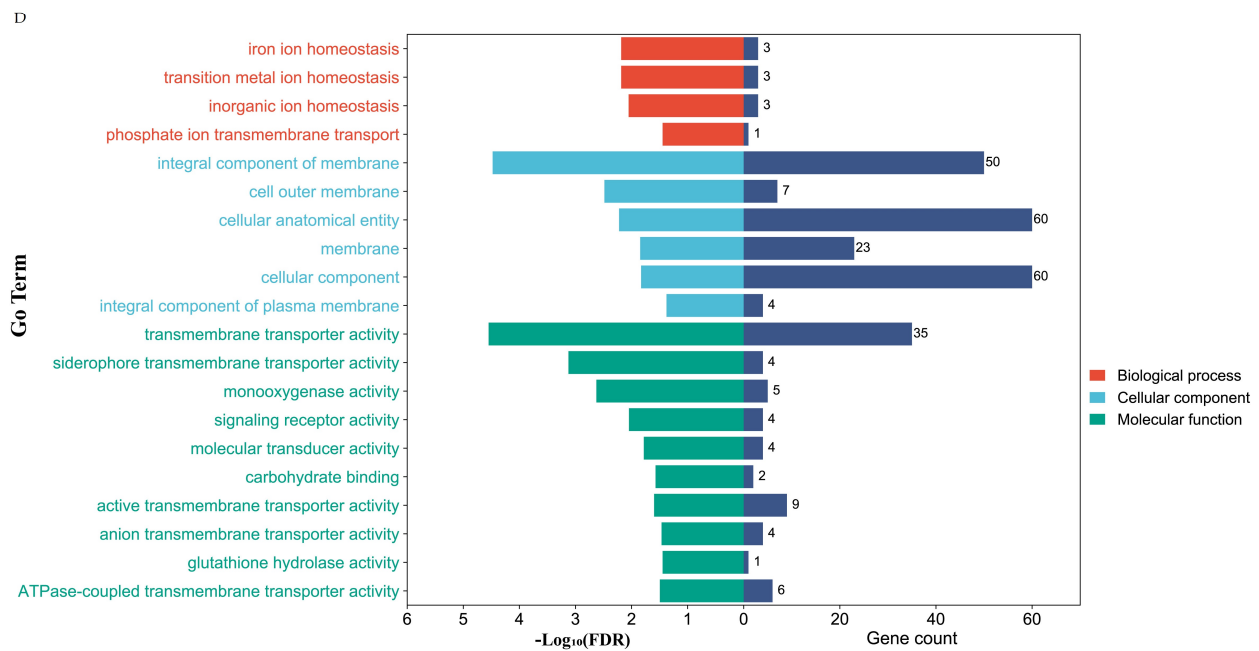


Figure 3. Comparative transcriptomic analysis between wild-type strain and $\Delta fliL$ strain of *P. plecoglossicida*. (A) Volcano map of transcriptome gene expression; (B) KEGG enrichment analysis of differentially expressed genes (DEGs); (C) KEGG functional enrichment chord diagram; (D) GO enrichment analysis of DEGs.

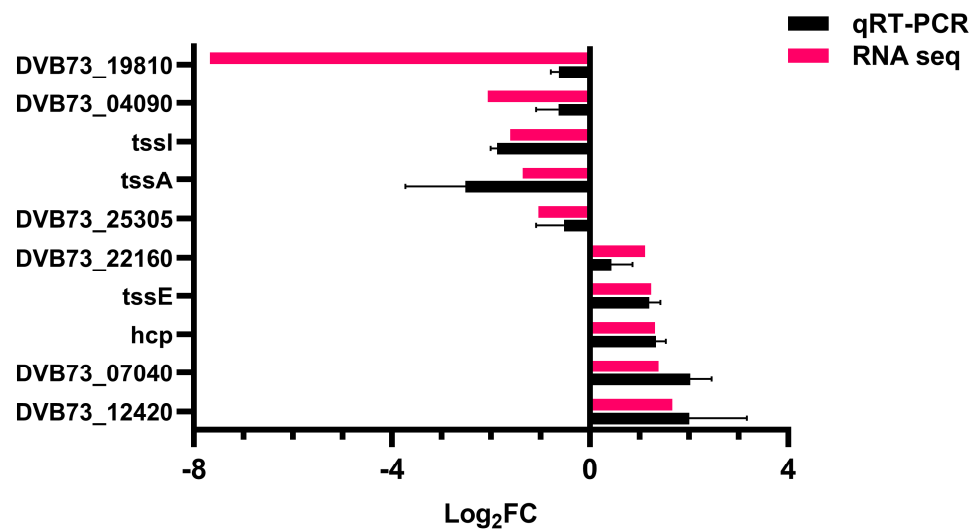


Figure 4. qRT-PCR validation of transcriptome. The vertical coordinate shows the name of the gene, and the horizontal coordinate shows the multiple of expression difference.

The differential genes were analyzed by GO enrichment and KEGG pathway to further explore the effect of *fliL* gene deletion on the transcriptome of *P. plecoglossicida*. The GO enrichment analysis with GOATOOLS software showed that there are three types of GO enrichment functions: molecular function (MF), cellular component (CC), and biological process (BP). A total of 44 GO pathways were enriched, 42 of which were significantly enriched. The 20 GO pathways with the highest degree of enrichment are shown in Figure 3D, among which the top 5 are the intrinsic component of membrane, an integral component of cytoplasm, transporter activity, transmembrane transporter activity, and siderophore uptake transmembrane transporter activity. It is suggested that the deletion of the *fliL* gene may affect the membrane and transmembrane transport activity of *P. plecoglossicida*. KEGG Pathway enrichment analysis showed that 35 differential

genes (DEGs) were enriched into 39 pathways in the KEGG database. Among them, 29 pathways downregulate differential gene enrichment, including the ABC transporter, flagellar assembly, biofilm formation, bacterial secretion system, and two-component system, etc. The top 20 enrichment pathways are shown in Figure 3B, and the genes corresponding to the top 10 KEGG pathways and their expression levels are shown in Figure 3C. It was noteworthy that the ABC transporter receptor pathway was the most significant pathway of enrichment. As one of the largest protein superfamilies, ABC transporters transport a variety of substrates across the cellular membranes of bacteria by ATP binding and hydrolysis (Figure 5A). The ABC transporter receptor pathway was analyzed, and its upregulation and downregulation are shown in Figure 5B. As shown in the Figure 5, the alkanesulfonate-binding protein (SsuA), ABC transporter permease (SsuC), and SsuB transporter are all downregulated. AfuB transporters in the iron uptake system and ZnuA and ZnuB transporters in the zinc uptake system were downregulated. In addition, the phosphate transport system permease protein PstA, methionine uptake transporter MetNI, and the urea permease UrtA, UrtC were also downregulated. The results showed that the transport and absorption ability of the Δ *fliL* strain to the outside world were weakened.

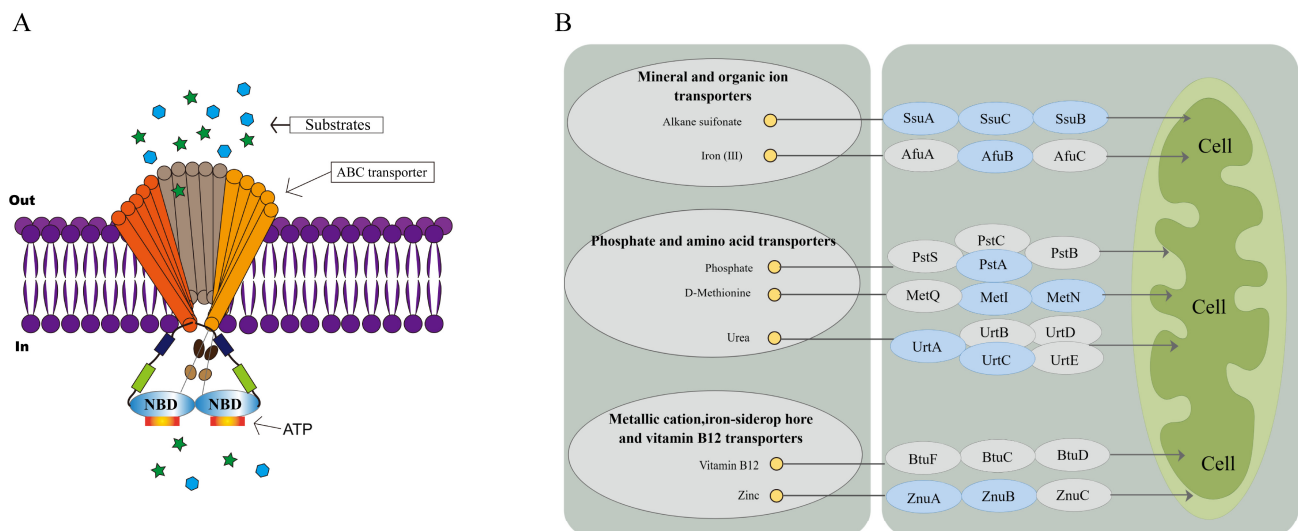


Figure 5. ABC transporter transport diagram. (A) ABC receptor transport substance simulation; (B) ABC transport path diagram: blue means downward adjustment, gray means no significant difference.

4. Discussion

As an important gene modification technology, gene knockout technology is widely used in the fields of animals and plants [30–32] and microorganisms [33–35]. It is one of the most powerful tools for studying the function of biological genes. The main methods include homologous recombination, the ZFN technique, TALEN technique, and CRISPR/Cas9 system mediation [36–38]. Homologous recombination has played a role in the study of a variety of bacteria. Examples of strains were *Bifidobacterium longum* [39], *Helicobacter pylori* [40], *Mycobacterium avium* subspecies *paratuberculosis*, (MAP) [41]. In this study, the *fliL* gene of *P. percoglossicida* was knocked out by homologous recombination of suicide plasmids, and the Δ *fliL* strain was constructed successfully, which laid the foundation for this study.

Most bacteria-infected hosts undergo four processes: contact, adhesion, entry, and host colonization [42], which are closely related to flagellar movement, biofilm formation, adhesion ability, and other virulence factors [43,44]. Flagellar movement is crucial to the survival and virulence of many pathogenic bacteria [17] and is one of the determinants of pathogenicity. The flagellar structure consists of three parts: a rotary motor, a universal joint,

and a helical propeller [45], which consists of more than 50 genes with multiple operons that regulate flagella synthesis and function [46]. For example, the *fliK* gene controls the length of flagellar hooks and is crucial for the motility of *Bacillus thuringiensis* [47]. In the study of *P. percoglossicida*, the silence of genes such as *fliG*, *flgK*, and *flgC* that encode flagellin all lead to a significant decline in the movement, adhesion, and biofilm formation of *P. percoglossicida* [10,14,15]. The survival rate of infected *Epinephelus coioides* increased by 55%, 55%, and 80%, respectively. These results suggest that flagella genes play a key role in the pathogenicity of bacteria. In this study, we used a homologous recombination technique to knock out the flagellum-related gene *fliL*. The biological characterization showed that the motility, adhesion, and biofilm-forming ability of $\Delta fliL$ strain were obviously decreased, but it has no effect on the growth of *P. percoglossicida*. By supplementing the *fliL* gene, the C- $\Delta fliL$ strain has regained its motility, and its biofilm-forming ability has also been improved. These results suggest that the *fliL* gene may be involved in the regulation of flagella assembly, thus weakening the virulence of the *P. percoglossicida*. The virulence of $\Delta fliL$ strain was reduced 12-fold compared to the wild-type strain by testing the median lethal dose (LD₅₀) of the infected pearl gentian grouper. Moreover, it was found that the virulence of C- $\Delta fliL$ strain was significantly greater than $\Delta fliL$ strain.

Bacterial virulence is regulated by a variety of factors besides flagella. Studies have shown that the bacterial outer membrane proteins OmpF and OmpA contribute to swimming motility and biofilm formation in *Citrobacter werkmanii* [48,49]. Ferredoxin receptor FusA is involved in iron transport, and knocking out the *fusA* gene significantly reduced the biofilm formation and adhesion ability of *P. percoglossicida*. The coregulation of flagella and other virulence factors on bacterial virulence is a complex mechanism that needs further study.

Transcriptomics is the study of the function of RNA transcripts. Transcriptome analysis can help us to study gene transcription and transcriptional regulation in cells at the overall level, which is the basis and starting point of gene function and structure research [50,51]. The transcriptome of prokaryotes adopts the chain-specific library building strategy [52,53]. The rapid development of this technology has promoted the research on the pathogenesis of pathogenic bacteria [54], and played an important role in the study of the drug resistance mechanism [55,56] and pathogenicity of pathogenic bacteria [57,58]. The $\Delta fliL$ strain in this study was different from the wild-type strain in the transcriptome level to some extent. A total of 126 genes with significant expression differences were screened in this transcriptome analysis, including 114 DEGs downregulated and 12 DEGs upregulated. The gene *fliK*, which is involved in flagella assembly, was significantly downregulated. Through enrichment analysis, the differential genes enriched into the GO pathway were mostly genes related to the membrane and transporter activity of bacteria, including those involved in the ferritic uptake of transporters. However, the absorption of manganese, iron, zinc, and other metal ions by bacteria is one of the key factors for their virulence [59–61]. There were 35 DEGs enriched ABC transporters, flagellar assembly, and the bacterial two-component system in the KEGG Pathway.

The ATP-binding cassette transporter family (ABC) transporter is a ubiquitous molecular pump [62] that can be classified as either an importer (type I and type II) or an exporter. Whereas type I and type II importers are found only in bacteria, whose role is to absorb essential nutrients, exporters transport molecules out of cells or organelles and exist in all organisms [63]. ABC exporters include type I secretory systems associated with the secretion of toxins, S-layer protein, siderophore, hydrolase, or antimicrobial peptide, which have roles in adhesion and colonization of the host. There are also glycoconjugates and polysaccharide biosynthetic pathways involved in membrane biosynthesis and immune escape. Importers are associated with nutrient acquisition (e.g., metal ions, amino acids, vitamins, and oligopeptides) and osmotic protection processes, all of which contribute significantly to bacterial pathogenicity [64]. In the transcriptome sequencing results of this study, the most significant pathway of KEGG enrichment was the ABC transport pathway, in which the expression of transporters for iron, zinc, and phosphate was significantly

downregulated. These results suggest that the deletion of the *fliL* gene weakens the transport system of *P. plecoglossicida* and affects its absorption of nutrients. This may be one of the reasons for the decreased virulence of the $\Delta fliL$ strain.

5. Conclusions

The *fliL* gene was related to the regulation of biofilm formation, migration, and adhesion ability of *P. plecoglossicida*. After the knockout of the *fliL* gene, the virulence of the strain was reduced 12-fold (LD₅₀ test), and the transcriptome of *P. plecoglossicida* was significantly affected. The *fliK* gene related to flagellar assembly and several genes related to transport were significantly downregulated, and the pathway enriched by differentially expressed genes was the ABC transporter. It suggests that the *fliL* gene might be influencing the *P. plecoglossicida*'s system of material transportation and flagellum assembly to reduce its virulence.

Supplementary Materials: The following supporting information can be downloaded at: <https://www.mdpi.com/article/10.3390/fishes8080397/s1>, Table S1: The primers used to construct strains. Table S2: Primer sequence for transcriptome validation. Figure S1: Electrophoretic diagram of the construction of the knockout strain. Figure S2: Electrophoretic diagram of the construction of the complement strain. Figure S3: Clustering analysis of differentially expressed genes.

Author Contributions: L.S.: performed experiments and data analysis, and completed the first draft. J.Z., L.Z. and Q.L.: provided useful help in the process of experiment and data analysis. L.H. and Y.Q.: provided guidance and supervised the process of developing the manuscript. Q.Y.: supervised, revised and edited the manuscript, and submitted the manuscript. All authors have read and agreed to the published version of the manuscript.

Funding: This work was supported by the Natural Science Foundation of Fujian Province under contract No. 2021J01828 and 2022J02044, National Natural Science Foundation of China under contract No. 31972836, Science and Technology Plan Project of Fuzhou City under contract No. 2022-P-014, Science and Technology Plan Project of Fujian Province under contract No. 2022L3059.

Institutional Review Board Statement: All animal protocols were approved by the Animal Ethics Committee of Jimei University (Acceptance No JMULAC201159).

Data Availability Statement: The original contributions presented in the study are included in the article/Supplementary Materials. Further inquiries can be directed to the corresponding authors.

Conflicts of Interest: The authors declare that the research was conducted in the absence of any commercial or financial relationships that could be construed as a potential conflict of interest.

References

1. Mzula, A.; Wambura, P.N.; Mdegela, R.H.; Shirima, G.M. Present Status of Aquaculture and the Challenge of Bacterial Diseases in Freshwater Farmed Fish in Tanzania; A Call for Sustainable Strategies. *Aquac. Fish.* **2021**, *6*, 247–253. [CrossRef]
2. Rodger, H.D. Fish Disease Causing Economic Impact in Global Aquaculture. In *Fish Vaccines*; Adams, A., Ed.; Birkhäuser Advances in Infectious Diseases; Springer: Basel, Switzerland, 2016; pp. 1–34. ISBN 978-3-0348-0980-1.
3. Wu, X.Y.; Xiong, J.B.; Fei, C.J.; Dai, T.; Zhu, T.F.; Zhao, Z.Y.; Pan, J.; Nie, L.; Chen, J. Prior exposure to ciprofloxacin disrupts intestinal homeostasis and predisposes ayu (*Plecoglossus altivelis*) to subsequent *Pseudomonas plecoglossicida*-induced infection. *Zool. Res.* **2022**, *43*, 648–665. [CrossRef]
4. Cai, H.Y.; Ma, Y.; Qin, Y.X.; Zhao, L.M.; Yan, Q.P.; Huang, L.X. Vvrr2: A New Vibrio ncRNA Involved in Dynamic Synthesis of Multiple Biofilm Matrix Exopolysaccharides, Biofilm Structuring and Virulence. *Aquaculture* **2023**, *563*, 738925. [CrossRef]
5. Du, Z.Y.; Zhang, M.M.; Qin, Y.X.; Zhao, L.M.; Huang, L.X.; Xu, X.J.; Yan, Q.P. The Role and Mechanisms of the Two-Component System EnvZ/OmpR on the Intracellular Survival of *Aeromonas hydrophila*. *J. Fish Dis.* **2022**, *45*, 1609–1621. [CrossRef] [PubMed]
6. Park, S.C.; Shimamura, I.; Fukunaga, M.; Mori, K.I.; Nakai, T. Isolation of Bacteriophages Specific to a Fish Pathogen, *Pseudomonas plecoglossicida*, as a Candidate for Disease Control. *Appl. Environ. Microbiol.* **2000**, *66*, 1416–1422. [CrossRef]
7. Xu, K.P.; Wang, Y.S.; Yang, W.X.H.; Cai, H.Y.; Zhang, Y.Y.; Huang, L.X. Strategies for Prevention and Control of Vibriosis in Asian Fish Culture. *Vaccines* **2022**, *11*, 98. [CrossRef]
8. Nishimori, E.; Kita-Tsukamoto, K.; Wakabayashi, H. *Pseudomonas plecoglossicida* Sp. Nov., the Causative Agent of Bacterial Haemorrhagic Ascites of Ayu, *Plecoglossus altivelis*. *Int. J. Syst. Evol. Microbiol.* **2000**, *50 Pt 1*, 83–89. [CrossRef]
9. Akayli, T.; Çanak, Ö.; Başaran, B. A New *Pseudomonas* Species Observed in Cultured Young Rainbow Trout (*Oncorhynchus mykiss* Walbaum, 1792): *Pseudomonas plecoglossicida*. *Biyol. Bilim. Araştırma Derg.* **2011**, *4*, 107–111.

10. Yuan, B.; Zhao, L.M.; Zhuang, Z.X.; Wang, X.R.; Fu, Q.; Huang, H.B.; Huang, L.X.; Qin, Y.X.; Yan, Q.P. Transcriptomic and Metabolomic Insights into the Role of the *flgK* Gene in the Pathogenicity of *Pseudomonas plecoglossicida* to Orange-Spotted Grouper (*Epinephelus coioides*). *Zool. Res.* **2022**, *43*, 952–965. [[CrossRef](#)]
11. Zhang, J.T.; Zhou, S.M.; An, S.W.; Chen, L.; Wang, G.L. Visceral Granulomas in Farmed Large Yellow Croaker, *Larimichthys crocea* (Richardson), Caused by a Bacterial Pathogen, *Pseudomonas plecoglossicida*. *J. Fish Dis.* **2014**, *37*, 113–121. [[CrossRef](#)]
12. Xin, G.; Zhao, L.M.; Zhuang, Z.X.; Wang, X.; Fu, Q.; Huang, H.B.; Huang, L.X.; Qin, Y.X.; Zhang, J.N.; Zhang, J.L.; et al. Function of the *rpoD* Gene in *Pseudomonas plecoglossicida* Pathogenicity and *Epinephelus coioides* Immune Response. *Fish Shellfish Immunol.* **2022**, *127*, 427–436. [[CrossRef](#)] [[PubMed](#)]
13. Tang, Y.; Jiao, J.P.; Zhao, L.M.; Zhuang, Z.X.; Wang, X.R.; Fu, Q.; Huang, H.B.; Huang, L.X.; Qin, Y.X.; Zhang, J.N.; et al. The Contribution of *exbB* Gene to Pathogenicity of *Pseudomonas plecoglossicida* and Its Interactions with *Epinephelus coioides*. *Fish Shellfish Immunol.* **2022**, *120*, 610–619. [[CrossRef](#)] [[PubMed](#)]
14. Jiao, J.P.; Zhao, L.M.; Huang, L.X.; Qin, Y.X.; Su, Y.Q.; Zheng, W.Q.; Zhang, J.N.; Yan, Q.P. The Contributions of *fliG* Gene to the Pathogenicity of *Pseudomonas plecoglossicida* and Pathogen-Host Interactions with *Epinephelus coioides*. *Fish Shellfish Immunol.* **2021**, *119*, 238–248. [[CrossRef](#)] [[PubMed](#)]
15. Yang, D.; Zhao, L.M.; Li, Q.; Huang, L.X.; Qin, Y.X.; Wang, P.; Zhu, C.Z.; Yan, Q.P. *flgC* Gene Is Involved in the Virulence Regulation of *Pseudomonas plecoglossicida* and Affects the Immune Response of *Epinephelus coioides*. *Fish Shellfish Immunol.* **2023**, *132*, 108512. [[CrossRef](#)] [[PubMed](#)]
16. Zhu, S.W.; Kumar, A.; Kojima, S.; Homma, M. FliL Associates with the Stator to Support Torque Generation of the Sodium-Driven Polar Flagellar Motor of *Vibrio*. *Mol. Microbiol.* **2015**, *98*, 101–110. [[CrossRef](#)]
17. Tachiyama, S.; Chan, K.L.; Liu, X.L.; Hathroubi, S.; Peterson, B.; Khan, M.F.; Ottemann, K.M.; Liu, J.; Roujeinikova, A. The Flagellar Motor Protein FliL Forms a Scaffold of Circumferentially Positioned Rings Required for Stator Activation. *Proc. Natl. Acad. Sci. USA* **2022**, *119*, e2118401119. [[CrossRef](#)]
18. Lin, T.S.; Zhu, S.W.; Kojima, S.; Homma, M.; Lo, C.J. FliL Association with Flagellar Stator in the Sodium-Driven *Vibrio* Motor Characterized by the Fluorescent Microscopy. *Sci. Rep.* **2018**, *8*, 11172. [[CrossRef](#)]
19. Lee, Y.Y.; Patellis, J.; Belas, R. Activity of *Proteus mirabilis* FliL Is Viscosity Dependent and Requires Extragenic DNA. *J. Bacteriol.* **2013**, *195*, 823–832. [[CrossRef](#)]
20. Mengucci, F.; Dardis, C.; Mongiardini, E.J.; Althabegoiti, M.J.; Partridge, J.D.; Kojima, S.; Homma, M.; Quelas, J.I.; Lodeiro, A.R. Characterization of FliL Proteins in *Bradyrhizobium diazoefficiens*: Lateral FliL Supports Swimming Motility, and Subpolar FliL Modulates the Lateral Flagellar System. *J. Bacteriol.* **2020**, *202*, e00708-19. [[CrossRef](#)]
21. Partridge, J.D.; Nieto, V.; Harshey, R.M. A New Player at the Flagellar Motor: FliL Controls Both Motor Output and Bias. *mBio* **2015**, *6*, e02367. [[CrossRef](#)]
22. Takekawa, N.; Isumi, M.; Terashima, H.; Zhu, S.W.; Nishino, Y.; Sakuma, M.; Kojima, S.; Homma, M.; Imada, K. Structure of *Vibrio* FliL, a New Stomatin-like Protein That Assists the Bacterial Flagellar Motor Function. *mBio* **2019**, *10*, e00292-19. [[CrossRef](#)] [[PubMed](#)]
23. Josenhans, C.; Suerbaum, S. The Role of Motility as a Virulence Factor in Bacteria. *Int. J. Med. Microbiol.* **2002**, *291*, 605–614. [[CrossRef](#)] [[PubMed](#)]
24. Suaste-Olmos, F.; Domenzain, C.; Mireles-Rodríguez, J.C.; Poggio, S.; Osorio, A.; Dreyfus, G.; Camarena, L. The Flagellar Protein FliL Is Essential for Swimming in *Rhodobacter sphaeroides*. *J. Bacteriol.* **2010**, *192*, 6230–6239. [[CrossRef](#)] [[PubMed](#)]
25. Ye, H.D.; Xu, Z.J.; Tao, Z.; Li, W.Y.; Li, Y.; Yang, A.; Wang, W.; Yin, X.L.; Yan, X.J. Efficacy and Safety of *Pseudomonas plecoglossicida* Mutant Δ tssD-1 as a Live Attenuated Vaccine for the Large Yellow Croaker (*Larimichthys crocea*). *Aquaculture* **2021**, *531*, 735976. [[CrossRef](#)]
26. Howery, K.E.; Rather, P.N. Allelic Exchange Mutagenesis in *Proteus mirabilis*. *Methods Mol. Biol.* **2019**, *2021*, 77–84. [[CrossRef](#)] [[PubMed](#)]
27. Vijayan, S.P.; Rekha, P.D.; Dinesh, U.; Arun, A.B. Determination of Acute Lethal Dose 50 (LD50) of Uranyl Nitrate in Male Swiss Albino Mice. *Res. J. Pharm. Technol.* **2018**, *11*, 1086. [[CrossRef](#)]
28. Melo Ferreira, R.; Sabo, A.R.; Winfree, S.; Collins, K.S.; Janosevic, D.; Gulbranson, C.J.; Cheng, Y.-H.; Casbon, L.; Barwinska, D.; Ferkowicz, M.J.; et al. Integration of Spatial and Single-Cell Transcriptomics Localizes Epithelial Cell-Immune Cross-Talk in Kidney Injury. *JCI Insight* **2021**, *6*, e147703. [[CrossRef](#)]
29. Rong, Y.; Tang, L.; Yin, H.F.; Sun, D.Y. A Modified Coriolis Method Was Used to Calculate the Number of BALB/cA-Nu Mice Treated with 1.2. LD50 of Dichloropropane. *Chin. J. Occup. Dis. Labor Hyg.* **2019**, *37*, 53–55.
30. Dong, Y.; Bai, H.T.; Dong, F.; Zhang, X.B.; Ema, H. Gene Knockout in Highly Purified Mouse Hematopoietic Stem Cells by CRISPR/Cas9 Technology. *J. Immunol. Methods* **2021**, *495*, 113070. [[CrossRef](#)]
31. Sasidharan, S.; Saudagar, P. Knockout of Tyrosine Aminotransferase Gene by Homologous Recombination Arrests Growth and Disrupts Redox Homeostasis in *Leishmania* Parasite. *Parasitol. Res.* **2022**, *121*, 3229–3241. [[CrossRef](#)]
32. Zhang, Y.X.; Zhang, Y.; Qi, Y.P. Plant Gene Knockout and Knockdown by CRISPR-Cpf1 (Cas12a) Systems. *Methods Mol. Biol.* **2019**, *1917*, 245–256. [[CrossRef](#)] [[PubMed](#)]
33. Choi, K.R.; Cho, J.S.; Cho, I.J.; Park, D.; Lee, S.Y. Markerless Gene Knockout and Integration to Express Heterologous Biosynthetic Gene Clusters in *Pseudomonas putida*. *Metab. Eng.* **2018**, *47*, 463–474. [[CrossRef](#)] [[PubMed](#)]

34. Han, X.; Tu, Y.Q.; Wu, H.; Zhang, L.J.; Zhao, S.N. Gene Knockout Revealed the Role of Gene FeoA in Cell Growth and Division of *Lactobacillus delbrueckii* Subsp. *Bulgaricus*. *Arch. Microbiol.* **2021**, *203*, 3541–3549. [[CrossRef](#)]
35. Zhu, X.W.; Wu, Y.K.; Lv, X.Q.; Liu, Y.F.; Du, G.C.; Li, J.H.; Liu, L. Combining CRISPR-Cpf1 and Recombineering Facilitates Fast and Efficient Genome Editing in *Escherichia coli*. *ACS Synth. Biol.* **2022**, *11*, 1897–1907. [[CrossRef](#)]
36. Carroll, D. Genome Engineering with Zinc-Finger Nucleases. *Genetics* **2011**, *188*, 773–782. [[CrossRef](#)] [[PubMed](#)]
37. Dalvie, N.C.; Lorgeree, T.; Biedermann, A.M.; Love, K.R.; Love, J.C. Simplified Gene Knockout by CRISPR-Cas9-Induced Homologous Recombination. *ACS Synth. Biol.* **2022**, *11*, 497–501. [[CrossRef](#)]
38. Kim, S.E.; Kim, J.W.; Kim, Y.J.; Kwon, D.N.; Kim, J.H.; Kang, M.J. Generation of Fibroblasts Lacking the Sal-like 1 Gene by Using Transcription Activator-like Effector Nuclease-Mediated Homologous Recombination. *Asian-Australas. J. Anim. Sci.* **2016**, *29*, 564–570. [[CrossRef](#)]
39. Sakaguchi, K.; He, J.L.; Tani, S.; Kano, Y.; Suzuki, T. A Targeted Gene Knockout Method Using a Newly Constructed Temperature-Sensitive Plasmid Mediated Homologous Recombination in *Bifidobacterium longum*. *Appl. Microbiol. Biotechnol.* **2012**, *95*, 499–509. [[CrossRef](#)]
40. Langford, M.L.; Zabaleta, J.; Ochoa, A.C.; Testerman, T.L.; McGee, D.J. In Vitro and in Vivo Complementation of the Helicobacter Pylori Arginase Mutant Using an Intergenic Chromosomal Site. *Helicobacter* **2006**, *11*, 477–493. [[CrossRef](#)]
41. Alonso, M.N.; Malaga, W.; Mc Neil, M.; Jackson, M.; Romano, M.I.; Guilhot, C.; Santangelo, M.P. Efficient Method for Targeted Gene Disruption by Homologous Recombination in *Mycobacterium avium* Subspecie *paratuberculosis*. *Res. Microbiol.* **2020**, *171*, 203–210. [[CrossRef](#)]
42. Chaussé, A.M.; Roche, S.M.; Moroldo, M.; Hennequet-Antier, C.; Holbert, S.; Kempf, F.; Barilleau, E.; Trottereau, J.; Velge, P. Epithelial Cell Invasion by *Salmonella typhimurium* Induces Modulation of Genes Controlled by Aryl Hydrocarbon Receptor Signaling and Involved in Extracellular Matrix Biogenesis. *Virulence* **2023**, *14*, 2158663. [[CrossRef](#)]
43. Prada, C.F.; Casadiego, M.A.; Freire, C.C. Evolution of *helicobacter* Spp: Variability of Virulence Factors and Their Relationship to Pathogenicity. *PeerJ* **2022**, *10*, e13120. [[CrossRef](#)] [[PubMed](#)]
44. Sano, G.; Takada, Y.; Goto, S.; Maruyama, K.; Shindo, Y.; Oka, K.; Matsui, H.; Matsuo, K. Flagella Facilitate Escape of *salmonella* from Oncotic Macrophages. *J. Bacteriol.* **2007**, *189*, 8224–8232. [[CrossRef](#)] [[PubMed](#)]
45. Tan, J.X.; Zhang, X.; Wang, X.F.; Xu, C.H.; Chang, S.; Wu, H.J.; Wang, T.; Liang, H.H.; Gao, H.C.; Zhou, Y.; et al. Structural Basis of Assembly and Torque Transmission of the Bacterial Flagellar Motor. *Cell* **2021**, *184*, 2665–2679.e19. [[CrossRef](#)] [[PubMed](#)]
46. Chilcott, G.S.; Hughes, K.T. Coupling of Flagellar Gene Expression to Flagellar Assembly in *Salmonella enterica* Serovar Typhimurium and *Escherichia coli*. *Microbiol. Mol. Biol. Rev.* **2000**, *64*, 694–708. [[CrossRef](#)]
47. Attieh, Z.; Mouawad, C.; Rejasse, A.; Jehanno, I.; Perchat, S.; Hegna, I.K.; Økstad, O.A.; Kallassy Awad, M.; Sanchis-Borja, V.; El Chamy, L. The *fliK* Gene Is Required for the Resistance of *Bacillus thuringiensis* to Antimicrobial Peptides and Virulence in *Drosophila melanogaster*. *Front. Microbiol.* **2020**, *11*, 611220. [[CrossRef](#)]
48. Zhou, G.; Wang, Y.S.; Peng, H.; Liu, H.Z.; Feng, J.; Li, S.J.; Sun, T.L.; Li, C.L.; Shi, Q.S.; Xie, X.B. Outer Membrane Protein of OmpF Contributes to Swimming Motility, Biofilm Formation, Osmotic Response as Well as the Transcription of Maltose Metabolic Genes in *Citrobacter werkmanii*. *World J. Microbiol. Biotechnol.* **2023**, *39*, 15. [[CrossRef](#)]
49. Zhou, G.; Wang, Y.S.; Peng, H.; Li, S.J.; Sun, T.L.; Shen, P.F.; Xie, X.B.; Shi, Q.S. Roles of OmpA of *Citrobacter werkmanii* in Bacterial Growth, Biocide Resistance, Biofilm Formation and Swimming Motility. *Appl. Microbiol. Biotechnol.* **2021**, *105*, 2841–2854. [[CrossRef](#)]
50. Dong, Z.C.; Chen, Y. Transcriptomics: Advances and Approaches. *Sci. China Life Sci.* **2013**, *56*, 960–967. [[CrossRef](#)]
51. Wirka, R.C.; Pjanic, M.; Quertermous, T. Advances in Transcriptomics: Investigating Cardiovascular Disease at Unprecedented Resolution. *Circ. Res.* **2018**, *122*, 1200–1220. [[CrossRef](#)]
52. Creecy, J.P.; Conway, T. Quantitative Bacterial Transcriptomics with RNA-Seq. *Curr. Opin. Microbiol.* **2015**, *23*, 133–140. [[CrossRef](#)]
53. Siezen, R.J.; Wilson, G.; Todt, T. Prokaryotic Whole-Transcriptome Analysis: Deep Sequencing and Tiling Arrays. *Microb. Biotechnol.* **2010**, *3*, 125–130. [[CrossRef](#)] [[PubMed](#)]
54. James, K.; Cockell, S.J.; Zenkin, N. Deep Sequencing Approaches for the Analysis of Prokaryotic Transcriptional Boundaries and Dynamics. *Methods* **2017**, *120*, 76–84. [[CrossRef](#)] [[PubMed](#)]
55. Ahn, A.C.; Cavalca, L.; Colombo, M.; Schuurmans, J.M.; Sorokin, D.Y.; Muyzer, G. Transcriptomic Analysis of Two *Thioalkalivibrio* Species Under Arsenite Stress Revealed a Potential Candidate Gene for an Alternative Arsenite Oxidation Pathway. *Front. Microbiol.* **2019**, *10*, 1514. [[CrossRef](#)]
56. Roe, C.; Williamson, C.H.D.; Vazquez, A.J.; Kyger, K.; Valentine, M.; Bowers, J.R.; Phillips, P.D.; Harrison, V.; Driebe, E.; Engelthaler, D.M.; et al. Bacterial Genome Wide Association Studies (BGWAS) and Transcriptomics Identifies Cryptic Antimicrobial Resistance Mechanisms in *Acinetobacter baumannii*. *Front. Public Health* **2020**, *8*, 451. [[CrossRef](#)]
57. Lebreton, A.; Cossart, P. RNA- and Protein-Mediated Control of *Listeria monocytogenes* Virulence Gene Expression. *RNA Biol.* **2017**, *14*, 460–470. [[CrossRef](#)]
58. Zhou, J.W.; Zhao, H.Q.; Yang, H.; He, C.Y.; Shu, W.; Cui, Z.L.; Liu, Q.Z. Insights into the Impact of Small RNA SprC on the Metabolism and Virulence of *Staphylococcus aureus*. *Front. Cell. Infect. Microbiol.* **2022**, *12*, 746746. [[CrossRef](#)]
59. Papp-Wallace, K.M.; Maguire, M.E. Manganese Transport and the Role of Manganese in Virulence. *Annu. Rev. Microbiol.* **2006**, *60*, 187–209. [[CrossRef](#)] [[PubMed](#)]

60. Wandersman, C.; Delepelaire, P. Bacterial Iron Sources: From Siderophores to Hemophores. *Annu. Rev. Microbiol.* **2004**, *58*, 611–647. [[CrossRef](#)]
61. Zheng, C.K.; Qiu, J.; Zhai, Y.M.; Wei, M.; Zhou, X.H.; Jiao, X.N. ZrgA Contributes to Zinc Acquisition in *Vibrio Parahaemolyticus*. *Virulence* **2023**, *14*, 2156196. [[CrossRef](#)]
62. Kieuvongngam, V.; Chen, J. Structures of the Peptidase-Containing ABC Transporter PCAT1 under Equilibrium and Nonequilibrium Conditions. *Proc. Natl. Acad. Sci. USA* **2022**, *119*, e2120534119. [[CrossRef](#)] [[PubMed](#)]
63. Beis, K. Structural Basis for the Mechanism of ABC Transporters. *Biochem. Soc. Trans.* **2015**, *43*, 889–893. [[CrossRef](#)] [[PubMed](#)]
64. Lewis, V.G.; Ween, M.P.; McDevitt, C.A. The Role of ATP-Binding Cassette Transporters in Bacterial Pathogenicity. *Protoplasma* **2012**, *249*, 919–942. [[CrossRef](#)] [[PubMed](#)]

Disclaimer/Publisher’s Note: The statements, opinions and data contained in all publications are solely those of the individual author(s) and contributor(s) and not of MDPI and/or the editor(s). MDPI and/or the editor(s) disclaim responsibility for any injury to people or property resulting from any ideas, methods, instructions or products referred to in the content.